Electronic Supplementary Material (ESI) for Journal of Materials Chemistry C.

Supplementary materials for

Ultrawide-frequency Electromagnetic-Wave Absorption Based on $FeCoNiCu_xMn$ High Entropy Alloys Synthesized through Swing Ball-milling

Haoran Zhou[a], Linwen Jiang[a,*], Lei Jia[a], Zhuo Tang[a], Lingling Wang[a], Anhua Wu[b], Xiaofeng Zhang[c*]

[a] School of Materials Science and Chemical Engineering, State Key Laboratory Base of Novel Functional Materials and Preparation Science, Ningbo University, Ningbo 315211, PR China

[b] Shanghai Institute of Ceramics, Chinese Academy of Sciences, Shanghai 201800, PR China

[c] Institute of New Materials, Guangdong Academy of Science, National Engineering Laboratory for Modern Materials Surface Engineering Technology, Guangzhou 510651, PR China

*Corresponding author:

jianglinwen@nbu.edu.cn (L. W. Jiang); zxf200808@126.com (X. F. Zhang).

$$\Omega = \frac{T\Delta S_{mix}}{|\Delta H_{mix}|} \quad \text{(S1)}$$

$$VEC = \sum_{i}^{n} c_i (VEC)_i \quad \text{(S2)}$$

$$\delta = \sqrt{\sum_{i=1}^{n} c_i \left(1 - r_i / \bar{r}\right)^2} \quad \text{(S3)}$$

Where c_i is the mole fraction of element i. $\bar{r}$ and T_m are the average atomic radius and the melting point of the alloy, respectively. The ΔH_{ij}^{mix} represents the mixing enthalpy of a binary system of equimolar composition in the liquid phase. The detailed data of parameters are listed in Table S1 and S2.

Tab. S1 Binary mixing enthalpies for each atom pair in–Fe–Co–Ni–Cu–Mn-B alloys.

ΔH_{ij}^{mix} **(kJ×mol^{-1})**					
Cu	4	13	6	4	0
/	Mn	0	-5	-8	-32
/	/	Fe	-1	-2	-26
/	/	/	Co	0	-24
/	/	/	/	Ni	-24
/	/	/	/	/	B

Tab. S2 Melting point, crystal structure and atomic radius.

Element	**Fe**	**Co**	**Ni**	**Cu**	**Mn**	**B**
Melting point (K)	1811.15	1768.15	1728.15	1357.75	1519.15	2349.15
Atomic radius (pm)	126	125	124	128	127	90

The powders prepared by the high-frequency swing ball-milling are of flake shape with uniform size distribution, as shown in Figs. 1(a)-(f). Due to the good ductility of Cu, it can be seen from the distribution histogram that the sample particle sizes are still in 0-20 μm with the increase of Cu contents, but the number of large size particles increased. EDS was used to characterize the element distribution of sample C2 with low Cu content and C6 with high Cu content, as shown in Fig. S2(a) and (b), respectively. The five elements were evenly distributed, except for the Cu element in the C6 sample, which has a high mixing enthalpy with the other four main elements and is very susceptible to segregation (Cu enrichment) at a high content.

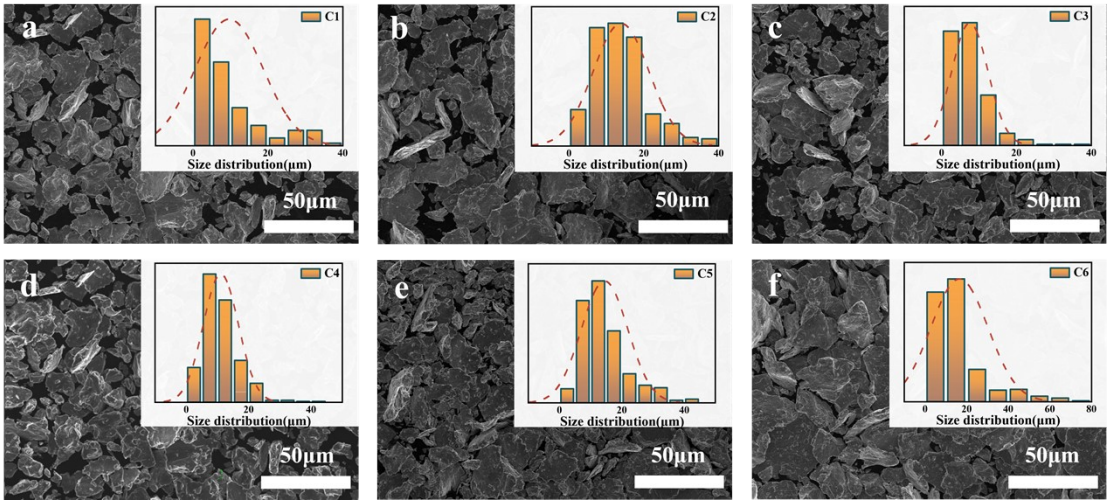

Fig. S1. (a-f) SEM images and size distribution histogram of (a) C1, (b) C2, (c) C3, (d) C4, (e) C5 and (f) C6.

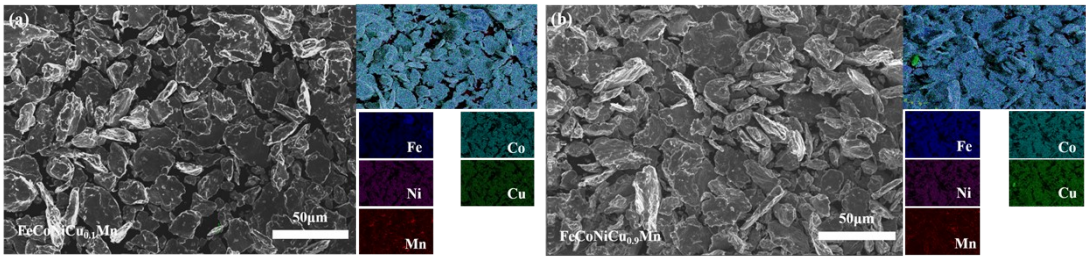

Fig. S2. Elemental mapping images of samples (a) C2 and (B) C6.

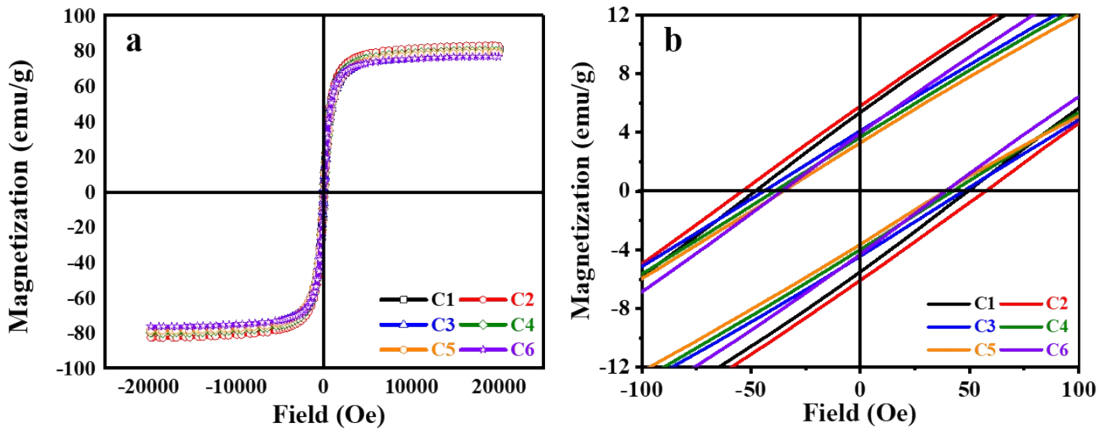

Fig. S3. (a) Hysteresis loops of $FeCoNiCu_xMn$ (x = 0, 0.1, 0.3, 0.5, 0.7 and 1.0) measured at an applied magnetic field range of −20,000 Oe to 20,000 Oe. (b) The zoomed region of magnetic hysteresis loops near origin.

Tab. S3 Electrochemical parameters of equivalent circuit under different stray current density.

Samples	R_s (Ω cm^2)	R_t	CPE1-T ($\mu\Omega^{-1}$ cm^2 s^p)	CPE1-P (F/cm)	R_{ox} (Ω cm^2)	CPE2-T ($\mu\Omega^{-1}$ cm^2 s^p)	CPE2-P (F/cm)
C1	1.934	191.90	0.00034143	0.66969	11141	0.00035281	0.8057
C2	3.885	74.13	0.00014257	0.71157	8387	0.00021383	0.85088
C3	3.432	31.01	0.00011395	0.74334	10032	0.00021001	0.8606
C4	4.047	37.24	0.00021770	0.70175	5242	0.00022326	0.86027
C5	4.066	48.14	0.00019731	0.80791	4282	0.00017672	0.70457
C6	4.283	92.77	0.00017291	0.67537	7407	0.00021109	0.84194
C7	2.977	50.18	0.00022577	0.74733	8125	0.00020569	0.78808

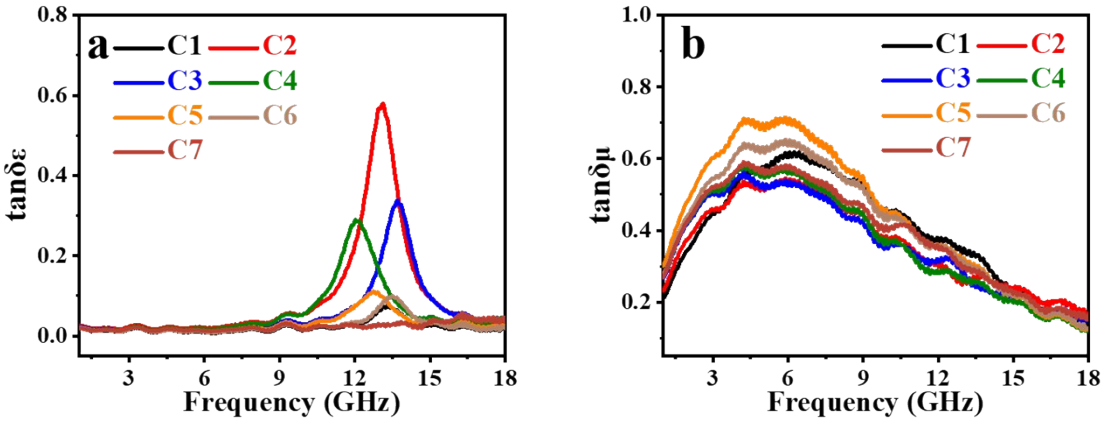

Fig. S4. (a) Dielectric loss factor and (b) magnetic loss factor of samples.

Tab. S4 Comparation of corrosion-resistance performances of different HEAs. [1-6]

Alloy	Solution	i_{corr} (μA/cm^2)	E_{corr} (V_{SCE})	Ref.
FeCoNiCu	3.5 wt.% NaCl	5.04	-0.364	1
FeCoNiCu	3.5 wt.% NaCl	5.78	-0.430	2
$FeCoNiAl_{0.3}$	3.5 wt.% NaCl	5.02	-0.204	3
FeCoNiCrBSiNb	3.5 wt.% NaCl	5.2	-0.390	4
$Ti_{21.6}Al_{11.3}Cr_{19.4}Si_{23.5}V_{22.0}O_{2.2}$	3.5 wt.% NaCl	6.14	-0.541	4
$FeCoNiCuAlCe_{0.01}$	3.5 wt.% NaCl	5.27	-0.430	2
$FeCoNiCuAlCe_{0.03}$	3.5 wt.% NaCl	4.61	-0.430	2
$FeCoNiCuAlCe_{0.09}$	3.5 wt.% NaCl	4.01	-0.450	2
AlCuCrFeMn	3.5 wt.% NaCl	6.97	-0.892	5
$AlCuCrFeMnW_{0.05}$	3.5 wt.% NaCl	6.12	-0.876	5
$AlCuCrFeMnW_{0.1}$	3.5 wt.% NaCl	5.39	-0.716	5
$AlCuCrFeMnW_{0.5}$	3.5 wt.% NaCl	4.32	-0.503	5
$AlCuCrFeMnW_{1.0}$	3.5 wt.% NaCl	3.32	-0.313	5
$FeCoNiCrMnAl_{0.5}$	3.5 wt.% NaCl	9.56	-0.428	6
$FeCoNiCu_{0.1}Mn$	3.5 wt.% NaCl	2.31	-0.098	This work

Tab. S5 Comparison of EMA performances with the related materials. [7-13]

Samples	Thickness (mm)	RL_{min} (dB)	EAB (GHz)	Ref.
$FeCoNiCrCuAl_{0.3}$@air@Ni-NiO	1.30	-41.40	4.00	7
FeCoNiCrAl	1.50	-35.30	2.70	8
$FeCoNiCrCuAl_{0.3}$	1.70	-40.20	4.48	9
$FeCoNiCuC_{0.04}$	1.72	-61.10	5.10	10
$FeCoNiCuC_{1.0}$	3.56	-59.90	5.20	10
$FeCoNiCuTi_{0.2}$	2.16	-47.80	4.76	11
FeCoNiCuAl	2.00	-19.70	2.50	12
FeCoNiTiCr@C	4.50	-20.43	2.50	13
FeCoNiTiV@C	4.50	-26.43	2.95	13
FeCoNiCrCu@C	2.00	-20.82	3.00	13
$FeCoNiCu_{0.1}Mn$	2.79	-71.0	6.79	This work

References

1. Y. A. Shen, H. M. Hsieh, S. H. Chen, J. Li, S. W. Chen and H. Nishikawa, *Appl. Surf. Sci.*, 2021, **546**, 148931.

2. Z. Wu, B. Li, M. Chen, Y. Yang, R. Zheng, L. Yuan, Z. Li, X. Tan and H. Xu, *J. Alloys Compd.*, 2022, **901**, 163665.

3. X. Yan, H. Guo, W. Yang, S. Pang, Q. Wang, Y. Liu, P. K. Liaw and T. Zhang, *J. Alloys Compd.*, 2021, **860**, 158436.

4. H. Zhang, W. Li, H. Xu, L. Chen, J. Zeng, Z. Ding, W. Guo and B. Liu, *Coatings*, 2022, **12**, 628.

5. D. Kumar, O. Maulik, V. Sharma, Y. Prasad and V. Kumar, *J. Mater. Eng. Perform.*, 2018, **27**, 4481-4488.

6. X. Mao, Y. Wang, J. Jiang, Y. Chi, Y. Dong and Y. Yang, *Mater. Lett.*, 2022, **314**, 131855.

7. H. Wu, D. Lan, B. Li, L. Zhang, Y. Fu, Y. Zhang and H. Xing, *Compos. Part B-Eng.*,

2019, **179**, 107524.

8. P. Yang, Y. Liu, X. Zhao, J. Cheng and H. Li, *Adv. Powder Technol.*, 2016, **27**, 1128-1133.

9. D. Lan, Z. Zhao, Z. Gao, K. Kou, G. Wu and H. Wu, *J. Magn. Magn. Mater.*, 2020, **512**, 167065.

10. J. Yang, L. Jiang, Z. Liu, Z. Tang and A. Wu, *J. Mater. Sci. Technol.*, 2022, **113**, 61-70.

11. J. Yang, Z. Liu, H. Zhou, L. Jia, A. Wu and L. Jiang, *ACS Appl. Mater. Interfaces*, 2022, **14**, 12375-12384.

12. Y. Duan, Y. Cui, B. Zhang, G. Ma and T. Wang, *J. Alloys Compd.*, 2019, **773**, 194-201.

13. Y. Li, Y. Liao, L. Ji, C. Hu, Z. Zhang, Z. Zhang, R. Zhao, H. Rong, G. Qin and X. Zhang, *Small*, 2022, **18**, 2107265.